Journal of Basic and Applied Engineering Research
p-ISSN: 2350-0077; e-ISSN: 2350-0255; Volume 5, Issue 7; October-December, 2018, pp. 533-540

http://www.krishisanskriti.org/Publication.html

Studies on X-ray Peak Broadening and Optical Properties of the Synthesized Nano-meter Sized Zinc Oxide Particles

Monalisha Goswami[1*], Nirab C. Adhikary [2] and Suparna Bhattacharjee[3]

[1,3]Department of Applied Sciences, Gauhati University, Guwahati-781014, Assam, India
[2]Physical Sciences Division, Institute of Advanced Study in Science and Technology, Paschim Boragaon, Garchuk, Guwahati-781035, Assam, India
E-mail: [1]monalishagoswami@yahoo.com, [2]nirab.physics@gmail.com, [3]suparnabhattacharjee3@gmail.com

Abstract—*We report synthesis of Zinc Oxide Nano Particles (ZnO-NPs) by chemical precipitation method at low temperature. The resulting ZnO product are subjected to annealing at 600^{0}C for two hours and the as synthesized ZnO sample was characterized by X-ray Diffraction (XRD), Field Emission Scanning Electron Microscopy (FE-SEM), Transmission Electron Microscopy (TEM) and Fourier Transform Infrared (FTIR) Spectroscopy, Ultra Violet–visible (UV-vis) absorption spectroscopy and Photoluminescence (PL) spectroscopy respectively. The XRD result reveals the formation of hexagonal wurzite structure. SEM image shows that prepared ZnO-NPs are spherical in shape with little agglomeration. TEM image shows the crystalline nature of ZnO-NPs with particle size of ~25nm.The FTIR spectrum exhibits peak corresponding to the stretching vibration of ZnO. The Williamson-Hall (W-H) plot was performed to distinguish the effect of crystalline size-induced broadening and strain-induced broadening at Full Width Half Maximum (FWHM) of the XRD profile. The physical parameters such as strain, stress, and energy density were also estimated for the XRD peaks using W-H analysis with different models such as Uniform Density Model, Uniform Stress Deformation Model, Uniform Deformation Energy Density model and by Size-Strain Plot method. The average crystallite size estimated by Scherrer's formula, W-H analysis and SSP method and the particle size estimated from TEM analysis found to be inter correlated. UV-Vis analysis demonstrates blue shift in band gap of the synthesized ZnO-NPs. The room temperature PL spectrum shows UV emission peak at 390nm and broad visible emission peak at 646nm respectively for the excitation wavelength 320nm.*

Keywords*: ZnO-NPs; XRD; hexagonal wurzite structure; chemical precipitation; crystallinity; FWHM, W-H analysis, blue shift.*

1. INTRODUCTION

Zinc Oxide (ZnO) is one of the most important II-VI semiconductors which is used in diverse fields of application such as photo detector, optical modulator waveguides, varistors, gas sensors transparent conductors, chemical sensor, light emitting diode, solar cell, piezoelectric devices, transducer, photo catalytic agent etc[1-4]. It is because ZnO possesses many unique properties such as high exciton binding energy (60meV) at room temperature, wide and direct band gap energy (E_g=3.37eV) [2,4,5], non-toxicity, good chemical stability, high thermal stability [3]etc**.** Various morphologies of ZnO nanostructures successfully synthesized by different methods such as thermal decomposition [1],sol-gel combustion[6], reverse micelle [7],spray pyrolysis [8], hydrothermal growth [9-12], atomic layer deposition [13], chemical vapor deposition [14]**,**chemical precipitation [15-17]etc.

In a perfect crystal, the crystallinity extends infinitely in all directions. However, due to presence of variety of defects in the crystal, there is a deviation from perfect crystallinity, which results in broadening of the X-ray diffraction peaks of the materials. The two important properties such as the crystallite size and lattice strain can be investigated from the XRD peak width analysis. Both crystallite size and lattice strain affect the Bragg peak such that width and intensity of the peak increase and shift the 2θ peak position accordingly [9,18]. However, fitting the data accurately from the powder diffraction is complicated and hence indirect methods such as Williamson-Hall (W-H) method, pseudo-Voigt function, Rietveld refinement and Warren-Averbach analysis can be adopted [19]. Among these methods, W-H analysis is a simplified integral method, which clearly differentiates between size induced and strain induced broadening by considering the peak width as a function of 2θ[6]. This paper reports the synthesis of ZnO-NPs by adopting simple and cost effective chemical precipitation method at low temperature, followed by annealing at 600^{0}C for two hours. The structural property of the synthesized ZnO-NPs was investigated by XRD, SEM, TEM and FTIR respectively. Though a lot of literature is available on the synthesis of ZnO nanoparticles, a detailed study using W-H models on the synthesized ZnO-NPs annealed at high temperature 600^{0}C is not yet reported. Therefore, in this paper we have given the importance of W-H

plots and SSP method to evaluate the crystallite size of the synthesized ZnO-NPs from XRD profile taking into account, the contributions of important factors such as lattice strain effect on the X-ray peak broadening. The average crystallite size estimated by Scherrer's formula, W-H analysis and SSP method and particle size estimated from TEM measurement were then correlated. The physical parameters such as lattice strain, lattice deformation stress and lattice strain energy density are also calculated using different W-H models and SSP method. In addition, to get more information about the synthesized particles, optical properties were investigated using UV-vis and PL spectroscopies respectively.

2. EXPERIMENTAL DETAILS

2.1. Materials and Method

All chemicals were analytical grade reagents and used directly without any further purification. Zinc nitrate hexa hydrate [(Zn $(NO_3)_2$.$6H_2O$], (MW= 297.49 gm/mol, 99.0 %purity) and Sodium Hydroxide (NaOH), (MW=40gm/mol, 97% purity) were all procured from Merck, Mumbai, India. Double distilled water was used throughout the experiment. To synthesize ZnO-NPs, aqueous solution of 0.1mol Zn $(NO_3)_2.6H_2O$ was prepared by stirring at 60^0C for one hour. Then 0.2 mol NaOH solution was slowly added drop wise into the Zn $(NO_3)_2.6H_2O$ solution until pH 8.5 reached for the solution. The final solution was stirred continuously at 60^0C for one hour and the white precipitate so obtained, washed repeatedly with distilled water to remove any impurities present in it. The precipitate dried at 90^0C for several hours to obtain fine ZnO powder and then subjected to annealing at 600^0C for two hours.

2.2. Characterization

The crystallinity and crystal phases were determined by using X-ray Powder Diffractometer (Phillips, X'PERT PRO) with Cu K_α radiation (λ=1.5406Å) with a scan rate of 0.02^0/sec at the Bragg's angle ranging from 20^0 to 80^0. The surface morphology of the sample was observed by FE-SEM using FE-SEM ZEISS analyzer. The size and diffraction pattern of ZnO-NPs were obtained by TEM using JEM-2100 electron microscope operating at an accelerating voltage 200 kV. The functional groups present in the synthesized ZnO sample was ascertained by FTIR spectroscopy (FTIR, Perkin Elmer) at room temperature, using with KBr pellets, in the wave number range from 4000 to 400 cm^{-1}. Optical absorption spectrum was taken with double beam spectrophotometer (HITACHI model U-3210) in the wavelength range 200 -600nm. Photoluminescence (PL) was recorded at room temperature, on a HITACHI model F-2500 fluorescence spectrophotometer with an excitation wavelength of 320 nm.

3. RESULTS AND DISCUSSION

3.1. XRD analysis

XRD pattern of the prepared sample is shown in Fig.1. All the peaks are well matched with hexagonal wurzite structure of ZnO as reported in JCPDS card no 36-1451. No peaks corresponding to any other phases are detected which implies that the synthesized ZnO sample is highly pure. Further, the peaks are sharper and enhanced which confirms the formation of good crystallinity of the obtained product[19].The hexagonal wurzite structure of ZnO is characterized by interconnecting Zn^{2+} and O^{2-}tetrahedrally such that each Zn^{2+} ion is surrounded by four O^{2-} ions and vice-versa [20,21]. The interplanar distance d_{hkl} for the hexagonal crystal system is calculated using Bragg's law [22],

$$n\lambda = 2d_{hkl}\sin\theta \quad (1)$$

where n is the order of diffraction (for first order n=1)

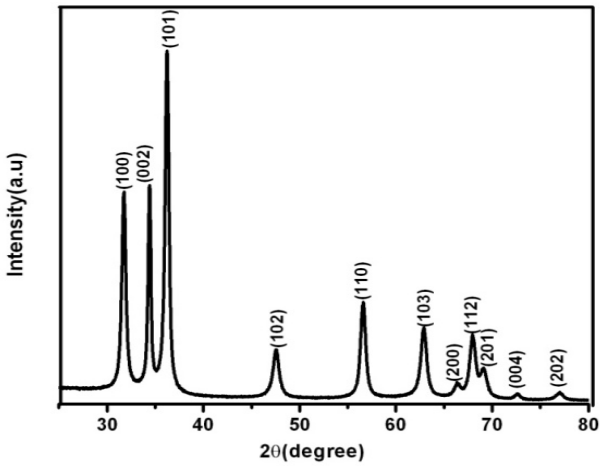

Fig. 1: X-ray diffraction pattern of ZnO-NPs annealed at 600^0C for 2 hours.

θ is the Bragg's angle, and λis the wavelength of X-ray. The calculated d_{hkl} values are 2.816 Å, 2.604 Å, 1.625Å and1.404Å.The lattice constants 'a' and 'c' and the volume 'V' of the unit cell are calculated using Lattice Geometric Equation [6], which is given as

$$\frac{1}{d^2_{hkl}} = \frac{4}{3}\left(\frac{h^2+hk+k^2}{a^2}\right)+\frac{l^2}{c^2} \quad (2)$$

$$V = \frac{\sqrt{3}}{2}a^2c \quad (3)$$

Combining Eqs. (1) and (2) we obtain

$$\frac{4\sin^2\theta}{\lambda^2} = \frac{4}{3}\left(\frac{h^2+hk+k^2}{a^2}\right)+\frac{l^2}{c^2}$$

$$\Rightarrow \sin^2\theta = \left(\frac{\lambda^2}{4a^2}\right)\left[\frac{4}{3}(h^2+hk+k^2)+\frac{l^2}{(c/a)^2}\right] \quad (4)$$

For the hexagonal system, the lattice constants a=b≠ c and crystallographic axes are $\alpha=\beta=90^0$ and $\gamma=120^0$. In the present study, having ascertained the hexagonal phase of prepared ZnO-NPs, 'a' is estimated from XRD peaks for which l=0 (i.e hk0) whereas 'c' is estimated from the XRD peaks for which h=k=0 (i.e 00l). Applying these conditions in Eq.(4), yields following expressions for 'a' and 'c' as

$$a=\frac{\lambda}{\sqrt{3}\sin\theta}\sqrt{h^2+hk+k^2} \quad (5)$$

$$c=\frac{\lambda}{2\sin\theta}l \quad (6)$$

Using Eqs. (5) and (6) the lattice constants a and c calculated only for those hkl indices which obey above conditions, are found to be a=3.2485 Å and c= 5.2062 Å (JCPDS card no.36-1451 a=3.2498 Å and c=5.2066 Å) respectively. Further, the volume 'V' of the unit cell calculated using Eq. (3) is 47.61 $(Å)^3$.

3.2. Estimation of crystallite size, strain and stress

3.2.1: Size by Scherrer analysis

The broadening of X-ray diffraction peak generally arises due to combined effect of instrumental broadening, broadening due to crystallite size and strain that may be present in the sample. Therefore, it is essential to correct the instrumental effect. The diffraction pattern from the line broadening of a standard material such as silicon was taken to correct the instrumental broadening. The instrumental corrected broadening β_{hkl} corresponding to each diffraction peak of ZnO was determined using the relation [19]

$$\beta^2_{hkl}=[(\beta^2)_{measured}-(\beta^2)_{instrumental}] \quad (7)$$

The average crystallite size (D) was estimated from the highest peak (101), using Debye-Scherrer's formula [23]

$$D=\frac{K\lambda}{(\beta_{hkl}\cos\theta)} \quad (8)$$

where K is a constant (K=0.9 for spherical shape),λ is the wavelength (=1.5406A^0) of Cu $K\alpha_1$ radiation, β is the full-width at half-maximum (FWHM) of the diffraction peak in radians and θ is the Bragg's diffraction angle respectively. The average crystallite size estimated for the synthesized ZnO sample found to be 12.6nm.The bond length (L) of Zn-O hexagonal crystal system is given as [3]

$$L=\sqrt{\left(\frac{a^2}{3}+\left(\frac{1}{2}-u^2\right)c^2\right)} \quad (9)$$

where u is the positional parameter in the wurtzite structure which gives the amount by which each atom is displaced with respect to the next along the 'c' axis. 'u' is given by the expression

$$u=\frac{a^2}{3c^2}+\frac{1}{4} \quad (10)$$

The Zn-O bond length calculated using Eq.(9) is found to be 1.9770 Å which is less than bulk ZnO (1.9778 Å). As reported in the literature [22], the difference in the bond length is attributed due to decrease in crystallite size of the synthesized ZnO sample.

3.2.2: Size and strain by W-H plot

Uniform Deformation Model (UDM)

In Williamson-Hall (W-H) method, the diffraction line broadening are considered both for size induced and strain induced broadenings and deconvoluting the peak width as a function of diffraction angle 2θ. The strain-induced broadening in the material due to crystal imperfection is calculated using the formula [19,24]

$$\varepsilon=\frac{\beta_s}{4\tan\theta} \quad (11)$$

where ε is the weighted average strain, β_s is the strain-induced broadening arising from crystal imperfect and θ is the Bragg's angle of different peaks.

Eqs. (8) and (11) reveal that the crystallite size varies as 1/cosθ and the strain varies as tanθ. That is, W-H method does not depend on 1/cosθ, instead varies as tanθ. Therefore, the total peak broadening is the sum of the contributions of broadenings due to crystallite size (β_D) and the strain(β_s), which is given by following mathematical expression

$$\beta_{hkl}=\beta_D+\beta_s \quad (12)$$

$$\Rightarrow\beta_{hkl}=\left(\frac{K\lambda}{D\cos\theta}\right)+(4\varepsilon\tan\theta)$$

$$\Rightarrow\beta_{hkl}\cos\theta=\left(\frac{K\lambda}{D}\right)+(4\varepsilon\sin\theta) \quad (13)$$

Eq.(13) is Williamson-Hall equation, which is known as Uniform Deformation Model (UDM). It assumes that strain is uniform in all crystallographic directions, thereby considering isotropic nature of the crystal. The W-H plot is drawn with 4sinθ along x-axis and $\beta_{hkl}\cos\theta$ along y-axis for the prominent diffraction peaks of the prepared ZnO sample (Fig.2). From the linear fit of the data, y-intercept gives the crystallite size D whereas strain ε is estimated from the slope of the fit. The plot shows a negative strain for the ZnO nanoparticles .This strain may be attributed to shrinkage of the ZnO lattice, which is observed in the calculated lattice constants values [6]. The estimated values of the crystallite size and strain obtained by the UDM model are 14nm and1.01 $x10^{-3}$ respectively.

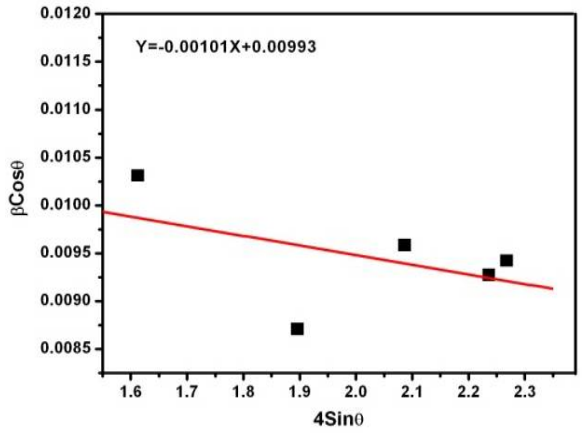

Fig. 2: The W-H analysis of ZnO nanoparticles annealed at 600^{0}C assuming UDM. Fit to the data, the strain is extracted from the slope and the crystalline size is extracted from the y-intercept of the fit.

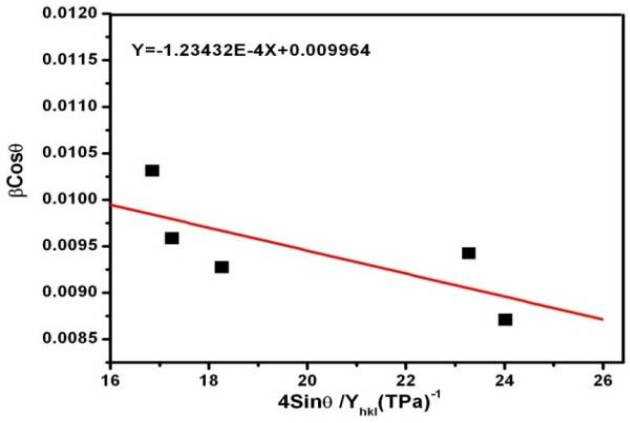

Fig. 3: The modified form of W-H analysis assuming USDM for ZnO-NPs annealed at 600^{0}C.Fit to the data, the stress is extracted from the slope and the crystallite size is extracted from the y-intercept of the fit.

Uniform Stress Deformation Model (USDM)

In USDM, it is assumed that the stress due to lattice deformation is uniform in all crystallographic directions and small micro strain might be present in the particles. In this model, strain is calculated from Hook's law, keeping only the linear proportionality between stress and strain, which is given as $\sigma=Y\varepsilon$, where σ is the stress of the crystal and Y is the Young's modulus of elasticity. This Hook's law is valid for very small strain. However, with the further increase of strain, the particles deviate from this linear proportionality [19]. Assuming that small strain is present in the prepared ZnO-NPs we can use Hook's law here. Applying Hook's law in Eq. (13), the modified form is as follows-

$$\beta_{hkl}\cos\theta=\left(\frac{K\lambda}{D}\right)+\left(\frac{4\sigma\sin\theta}{Y_{hkl}}\right) \quad (14)$$

Eq.(14) represents USDM, where Y_{hkl} is the Young's modulus in the direction perpendicular to the set of crystal lattice planes (hkl). On plotting $\left(\frac{4\sin\theta}{Y_{hkl}}\right)$ along x-axis and $\beta_{hkl}\cos\theta$ along y-axis the uniform deformation stress σ can be estimated from the slope of the line whereas the crystallite size D from the intercept. The strain ε can be determined if the values of Y_{hkl} are known. For hexagonal wurzite structure, the following relation [19, 23] gives Young's modulus, as

$$Y_{hkl}=\frac{\left[h^2+\frac{(h+2k)^2}{3}+\left(\frac{al}{c}\right)^2\right]^2}{S_{11}\left(h^2+\frac{(h+2k)^2}{3}\right)^2+S_{33}\left(\frac{al}{c}\right)^4+(2S_{13}+S_{44})\left(h^2+\frac{(h+2k)^2}{3}\right)\left(\frac{al}{c}\right)^2} \quad (15)$$

where $S_{11}(7.858\times10^{-12}m^2N^{-1})$, $S_{13}(-2.206\times10^{-12}m^2N^{-1})$, S_{33} $(6.940\times10^{-12}m^2N^{-1})$and $S_{44}(23.57\times10^{-12}m^2N^{-1})$ respectively are the elastic compliances of ZnO[22].The average value of Young's modulus (Y) for hexagonal ZnO-NPs estimated to be ~128 GPa which agrees well with the bulk ZnO [9]. Eq.15 represents USDM.

Fig.3 shows the plot of $\left(\frac{4\sin\theta}{Y_{hkl}}\right)$ vs $\beta_{hkl}\cos\theta$ for the prepared ZnO sample. The lattice deformation stress σestimated from the slope of the linear fit and the crystallite size D from the intercept on the y-axis are obtained as 123.4 MPa and 13.91nm respectively.

Uniform Deformation Energy Density Model (UDEDM)

The UDEDM is another model, which is used to determine the energy density of a crystal. Eq.(13)depicts that crystals are assumed to be uniform and homogeneous nature. However, this assumption of uniformity and homogeneity, in many cases, is not fulfilled. Further, the constants of proportionality in the relations between stress and strain are no longer independent if the strain energy density is taken into account. According to Hooke's law, the energy density u (energy per unit volume) is related to strain ε as $u=\varepsilon^2Y_{hkl}/2$ [9]. By substituting $\varepsilon=\sigma/Y_{hkl}$ in the equation for u, we obtain $u=\sigma^2/(2Y_{hkl})$. The modified form of Eq.(14) is given as

$$\beta_{hkl}\cos\theta=\left(\frac{K\lambda}{D}\right)+\left(4\sin\theta\left(\frac{2u}{Y_{hkl}}\right)^{1/2}\right) \quad (16)$$

A plot of $(\beta_{hkl}\cos\theta)$ vs$\left(4\sin\theta\left(\frac{2u}{Y_{hkl}}\right)^{1/2}\right)$ is shown in Fig.4. The energy density u and the crystallite size D estimated from the slope and the y-intercept of the linear fit of the data are found to be 13.53 nm and70kJm^{-3} respectively.

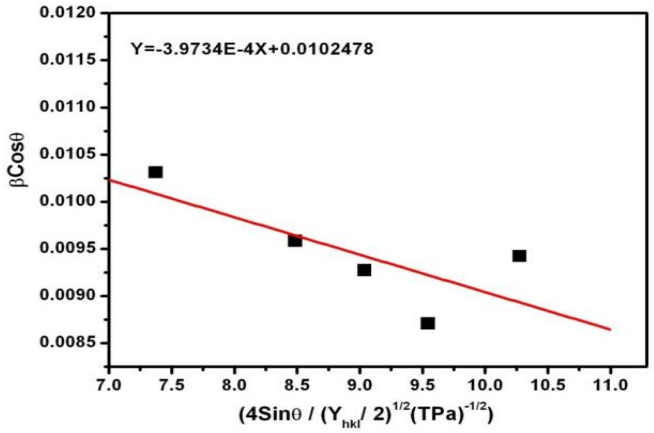

Fig. 4: The modified form of W-H analysis assuming UDEDM for ZnO-NPs annealed at 600^{0}C.Fit to the data, the energy density is extracted from the slope and the crystallite size is extracted from the y-intercept of the fit.

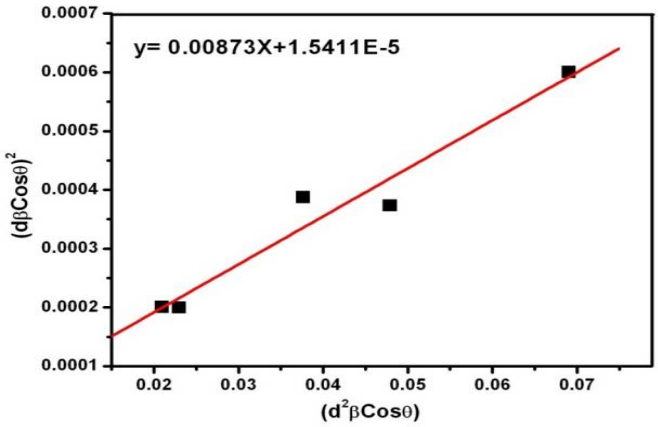

Fig. 5: The SSP plot of ZnO-NPs annealed at 600^{0}C. The crystallite size is estimated from the slope of the liner fitted data and the root of y-intercept gives the strain.

3.2.3: Size-Strain Plot method

The W-H plot has demonstrated that the line broadening was essentially isotropic. This implies that the diffracting domains were isotropic due to the contribution of micro strain. However, in case of isotropic line broadening, size-strain parameters can be better evaluated from the size-strain plot (SSP), which has a benefit that more importance is given to data from the reflections at low angles rather than those at higher angles where the precision is often lower. In this method, it is assumed that the ‘‘crystallite size” profile is described by a Lorentzian function and the ‘‘strain profile” by a Gaussian function [6] and is given as

$$(d_{hkl}\beta_{hkl}\cos\theta)^2=\frac{K}{D}(d^2_{hkl}\beta_{hkl}\cos\theta)+\left(\frac{\varepsilon}{2}\right)^2 \quad (17)$$

where K is a constant which depends on the shape of the particles. For spherical particle K=3/4. The SSP plot, shown in Fig.5, is obtained by taking the terms $(d^2_{hkl}\beta_{hkl}\cos\theta)$ and $(d_{hkl}\beta_{hkl}\cos\theta)^2$on x-axis and y-axis respectively for the all peaks of ZnO-NPs with the wurtzite hexagonal phase from $2\theta = 25^0$–80^0. In this case, the crystallite size D is determined from the slope of the linearly fitted data and the root of the y-intercept gives the strain (ε) which are obtained as 15.2nm and $0.7851\text{x}10^{-3}$ respectively.

3.3 Morphological studies

Fig. 6 shows the SEM image of the synthesized ZnO sample resulted from annealing at 600^{0}C, which demonstrates that particles are nearly spherical with little agglomeration, which is due to overlapping or aggregation of smaller particles at high annealing temperature. The result of EDX analysis of ZnO nanoparticles indicates that the ZnO-NPs contain 100% ZnO.

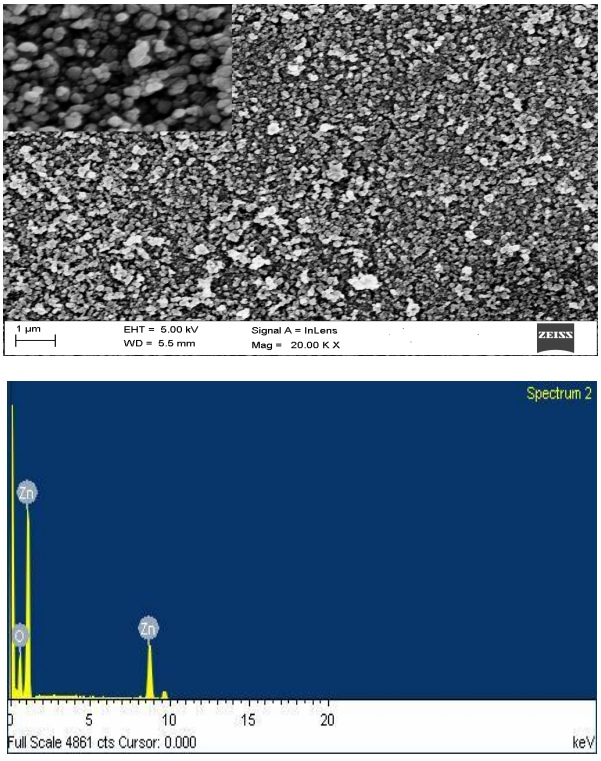

Fig. 6: SEM image and EDX spectrum of the synthesized ZnO-NPs annealed at 600^{0}C.

The TEM image shown in Fig.7 (a) reveals the formation of both hexagonal and circular shaped particles. Although the nanoparticles are slightly agglomerated, their grain boundaries are clearly distinguishable and the average particle size found to be 25±2nm.The corresponding SAED pattern shown in Fig. 7(b) indicates the crystalline nature of ZnO nanoparticles. The HRTEM image, Fig.7(c), clearly shows that the spacing between two adjacent lattice fringes is of 0.24 nm, which corresponds to the (101) plane of the wurtzite structure of ZnO.

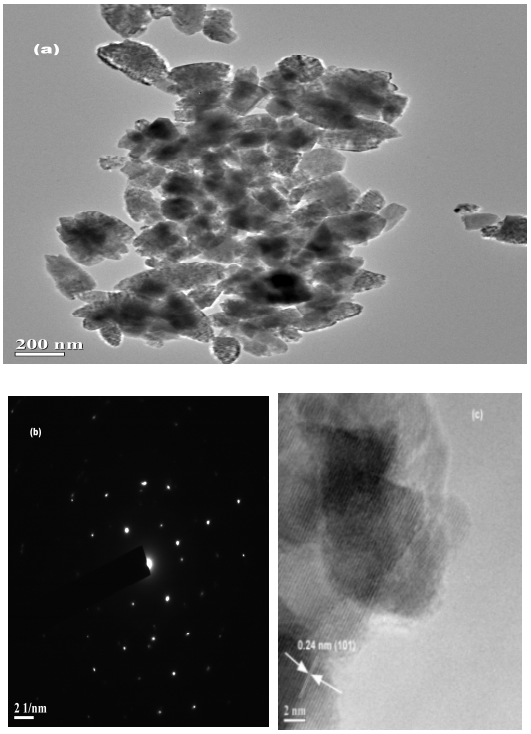

Fig. 7: (a) TEM image (b) SAED pattern and (c) HRTEM image of the prepared ZnO sample

The average crystallite size of the ZnO-NPs estimated from UDM,USDM ,UDEDM and SSP method found to be almost similar which implies that inclusion of strain has a very small effect on the average crystallite size. However, the average crystallite size estimated from Scherrer's method varies from W-H analysis, which is due to the difference in averaging the particle size distribution.

3.4 FTIR analysis

Figure 8 shows the FTIR spectrum of the synthesized ZnO sample annealed at 600^0C.The broad absorption peak observed at around 3429$cm^{-1}$and another peak around 1627 cm^{-1}correspond to O-H stretching and bending vibrations of surface adsorbed H_2O molecules [25]. A very weak and negligible absorption peak obtained at 2342 cm^{-1} can be attributed to the existence of CO_2 molecules in air [26]. The peaks observed at 1520 $cm^{-1}$and 940cm^{-1}can be assigned to asymmetric and symmetric stretching mode vibrations of Zinc carboxylate [27].The strong peak around 570 cm^{-1} indicates the formation of stretching mode of ZnO [28].

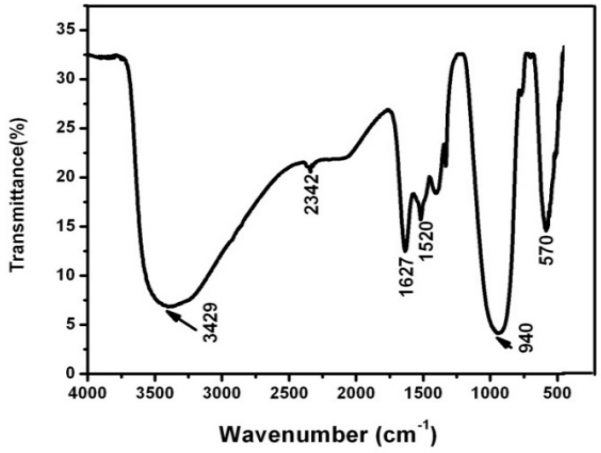

Fig.8: FTIR spectrum of the prepared ZnO sample annealed at 600^0C.

3.5 UV-Vis Absorption spectroscopy

The optical absorption spectrum of ZnO nanoparticles prepared under aqueous condition is shown in Fig.9 (a). It is observed that the excitonic absorption peak is at 301 nm, which can be attributed to the formation of lower crystallite size of the synthesized ZnO-NPs.

The optical band gap (E_g) can be calculated using Tauc's relation [4] which is given as

$$\alpha h\nu = B(h\nu - E_g)^n \quad (18)$$

where B is a constant, α is absorption coefficient(α=2.303A/t, A is the absorbance and t is the thickness of the cuvette), hν is the energy of the incident photon, n=2 and ½ depending upon the nature of electronic transition responsible for absorption and n=½ for direct transition.

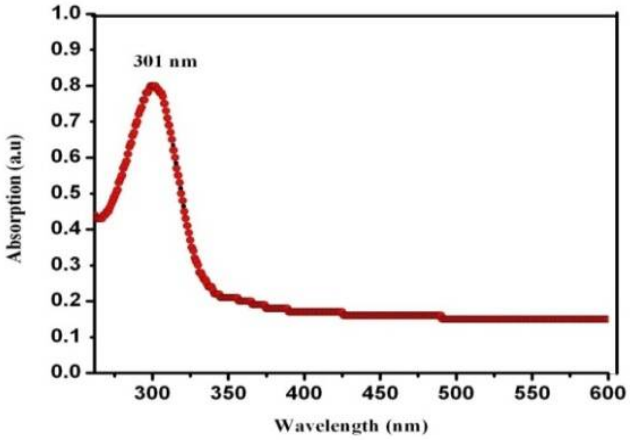

Fig. 9 (a): UV-vis absorption spectrum of synthesized ZnO nanoparticles.

Fig. 9 (b) presents the variation of $(\alpha h\nu)^2$ versus $h\nu$ for ZnO nanoparticles. The band gap value estimated by extrapolating the linear portion of the plot of $(\alpha h\nu)^2$ versus $h\nu$ to $(\alpha h\nu)^2=0$, found to be 3.78eV, which clearly implies the blue shift of the synthesized ZnO sample relative to the bulk ZnO (E_g=3.37eV)[2].

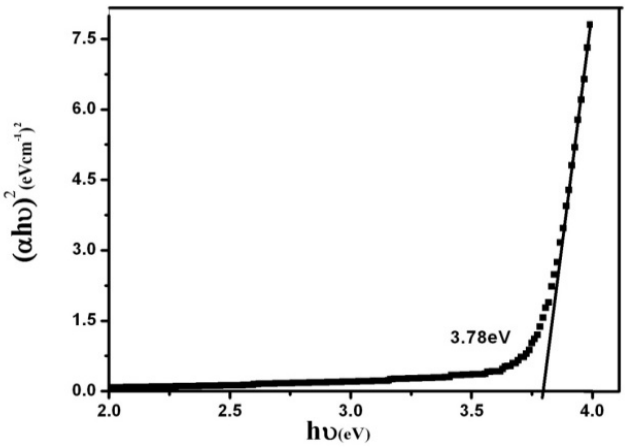

Fig. 9 (b): $(\alpha h\nu)^2$ versus $h\nu$ plot of synthesized ZnO-NPs.

3.6 Photoluminiscence

The photoluminescence (PL) spectroscopy is an effective method to investigate the presence of defects in the synthesized sample. Generally, PL spectrum shows two kinds of emission bands- one band, which lies in the UV region, is known as near -band-edge (NBE) emission and the other band located in the visible region is known as deep-level emission (DLE)[29]. The room temperature PL spectrum of the synthesized ZnO sample is shown in Fig.10. A UV emission peak observed at a wavelength of 390nm is related to near -band-edge (NBE) emission and is attributed to the process of recombination of free excitons of ZnO [1].

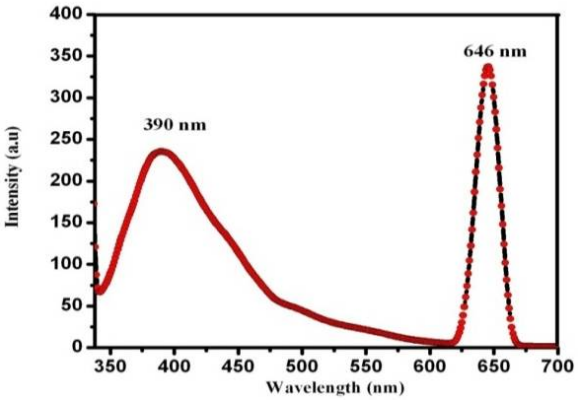

Fig. 10: Room temperature photoluminiscence spectrum of synthesized ZnO-NPs.

A strong visible emission peak positioned at ~646nm is also seen in the spectrum, which corresponds to red emission. Generally, emission in the visible region indicates the presence of intrinsic defects in the synthesized ZnO lattice [10]. Different intrinsic defects such as oxygen vacancy (V_O), zinc vacancy (V_{Zn}), zinc interstitial (Zn_i), oxygen interstitial (O_i), and oxygen antisite (O_{Zn}) may occur in the ZnO lattice [1]. In the present study, red emission might originate due to zinc vacancies or excess oxygen [30].

4. CONCLUSIONS

We have successfully synthesized ZnO nanoparticles by simple chemical precipitation method and characterized by XRD, SEM, TEM, FTIR, UV-Vis and PL respectively. XRD data reveals the formation hexagonal wurzite structure of ZnO. SEM image shows nearly spherical particles with little agglomeration. The FTIR spectrum exhibits peak at 570 cm^{-1}, which confirms the formation of ZnO. The blue shift observed in the UV-vis absorption spectrum clearly demonstrates the size confinement in ZnO nanocrystals. The PL spectrum analysis shows strong UV emission due to excitonic recombination along with intrinsic defects. The broadening of the X-ray peak of the synthesized ZnO sample, due to crystallite size and associated lattice strain were analyzed by Scherrer method, W-H models (UDM, USDM and UDEDM) and SSP method respectively. The average crystallite size found to be almost similar, indicating that induced strain has very little effect on the crystallite size of the ZnO. Further, using three W-H models and SSP method, we have estimated lattice deformation stress, strain and energy density values of the ZnO crystal.TEM image of the synthesized ZnO sample clearly indicates crystalline nature and the particle size obtained is in good agreement with the results of the W-H analysis and SSP method. It is found that W-H models (UDM, USDM and UDEDM) and SSP method are more accurate in determining the crystallite size and associated strain in comparison to Scherrer's method. The Scherrer's method estimates only the crystallite size and is not considering the peak broadening resulting from some important factors such as inhomogeneous lattice strain. Therefore, it can suggest that in determining the crystallite size of nano materials the contribution of instrumental effects as well as lattice strain on broadening of X- ray peak need to be considered.

5. ACKNOWLEDGMENT

Author Monalisha Goswami is greatly thankful to the Department of Applied Sciences, Gauhati University for providing laboratory facilities. The author is also thankful to SAIF, Department of Instrumentation and USIC, Gauhati University for XRD measurement, Department of Chemistry, Gauhati University for UV-vis, PL and FTIR studies, Tezpur University for SEM analysis and SAIF, North Eastern Hill University for TEM analysis.

REFERENCES

[1] Mishra, S. K., Srivastava R. K., Prakash S.G., "ZnO nanoparticles: Structural, optical and photoconductivity characteristics", *Journal of Alloys and Compounds, 539*, 19 June 2012, pp1-6.

[2] Hammiche L., Slimi O., Djouadi D., Chelouche A., Touam T., "Effect of supercritical organic solvent on structural and optical properties of cerium doped zinc oxide aerogel nanoparticles", *Optik, 145*, 2 August 2017, pp 448-455.

[3] Othman A.A., Osman M.A., Ibrahim E.M.M., Ali M. A., "Sonochemically synthesized ZnO nanosheets and nanorods: Annealing temperature effects on the structure, and optical properties", *Ceramics International 43*, 28 September 2016, pp527-533.

[4] Goswami M., Adhikary N. C., Bhattacharjee S., "Effect of annealing temperatures on the structural and optical properties of zinc oxide nanoparticles prepared by chemical precipitation method", *Optik 158*, 29 December 2017, pp 1006-1015.

[5] Escudero R., Escamilla R., "Ferromagnetic behavior of high-purity ZnO nanoparticles", *Solid State Communication 151*, 21 November 2010,pp 97-101.

[6] Zak A. K.,. Majid Abd. W.H., Abrishami M.E., Yousefi R., "X-ray analysis of ZnO nanoparticles by Williamsone Hall and size strain plot methods", *Solid State Sciences13*, 24 November 2010,pp 251-256.

[7] Mazhdi M., Saydi J., Karimi M., Seidi J., Mazhdi F., "A study on optical, photoluminescence and thermoluminescence propertiesof ZnO and Mn doped-ZnO nanocrystalline particles", *Optik 124*, 11 December 2012,pp 4128-4133.

[8] Edinger S., Bansal N., Bauch M., Wibowo R.A., Jvari G.U., Hamid R., Trimmeland G., Dimopoulos T., "Highly transparent and conductive indium-doped zinc oxide films deposited at low substrate temperature by spray pyrolysis from water-based solutions", *Journal of Material Science 52*, 20 April 2017, pp 8591-8602.

[9] Yogamalar R., Srinivasan R., Vinu A., Ariga K., Bose A. C., "X-ray peak broadening analysis in ZnO nanoparticles", *Solid State Communication, 149*, 30 July 2009,pp 1919-1923.

[10] Narayanan G. N, Ganesh R. S., Karthigeyan A., "Effect of annealing temperature on structural, optical and electrical properties of hydrothermal assisted zinc oxide nanorods", *Thin Solid Films 598*, 30 November 2015 pp39-45.

[11] Wirunmongkol T., O-Charoen N., Pavasupree S., "Simple hydrothermal preparation of zinc oxide Powders Using Thai autoclave unit", *Energy Procedia 34*,2013, pp 801-807.

[12] Holi A. M., Zainal Z., Talibd Z. A., Lim H.N., Yap C.C., Chang S. K., Ayal A. K., "Effect of hydrothermal growth time on ZnO nanorod arrays photoelectrode performance", *Optik127*, 5 September 2016, pp11111-11118.

[13] Tian J.L., Zhang H.Y., Wang G. G., Wang X.Z., Sun R., Jin L., Han J.C., "Influence of film thickness and annealing temperature on the structural and optical properties of ZnO thin films on Si (100)substrates grown by atomic layer deposition", *Super lattices and Microstructures 83*, 23 April 2015, pp719-729.

[14] Sharma V.K., Najim M., Srivastava A.K., Varma G.D., "Structural and magnetic studies on transition metal (Mn, Co) doped ZnO nanoparticles", *Journal of Magnetism and Magnetic Materials 324*, 17 September 2011, pp 683-689.

[15] Kumar S. S., Venkateswarlu P., Rao V. R., Rao G. N. , "Synthesis, characterization and optical properties of zinc oxide nanoparticles", *International Nano Letters*, 3, 07 May 2013 pp1-6.

[16] Bagheri S., Chandrappa K. G., Hamid S. B. A., "Facile synthesis of nano-sized ZnO by direct precipitation method", *Der Pharma Chemica 5*, 2013, pp 265- 270.

[17] Suntako R., "Effect of zinc oxide nanoparticles synthesized by a precipitation method on mechanical and morphological properties of the CR foam", *Bulletin of Material Science 38*, 22 July 2015, pp 1033-1038.

[18] Prabhu Y. T., Rao K. V., Sai Kumar V. S., Kumari B. S., "X-ray Analysis of Fe doped ZnO Nanoparticles by Williamson-Hall and Size-Strain Plot", *World Journal of Nano Science and Engineering, 4*, 16 December 2013, pp 21-28.

[19] Bindu P., Thomas S., "Estimation of lattice strain in ZnO nanoparticles: X-ray peak profile analysis", *Journal of Theoretical and Applied Physics 8*, 30 July 2014, pp 123-134.

[20]S.Baruah, J.Dutta, "Hydrothermal growth of ZnO nanostructures", *Science and Technology Advanced Material 10*, 13 January 2009, pp1-18.

[21]Sawyer S., Qin L., Shing C., "Zinc oxide nanoparticles for ultraviolet photodetection, International Journal of High Speed Electronic and System"20,2011,pp183-194.
DOI: 10.1142/S0129156411006519

[22] Sahai A., Goswami N., "Structural and vibrational properties of ZnO nanoparticles synthesized by the chemical precipitation method", *Physica E 58*, 17 December 2013, pp130-137.

[23] Mote V.D., Purushotham Y., Dole B.N., "Williamson-Hall analysis in estimation of lattice strain in nanometer-sized ZnO particles", *Journal of Theoretical and Applied Physics*, 2012, 6:6. doi:10.1186/2251-7235-6-6.

[24] Kahouli M., Barhoumi A., Bouzid A., Hajry A. Al., Guermazi S., "Structural and optical properties of ZnO nanoparticles prepared by direct precipitation method", *Superlattices and Microstructure, 85*, 15 May 2015,pp 7-23.

[25] Bhuyan B., Paul B., Purkayastha D.D., Dhar S. S., Behera S., "Facile synthesis and characterization of zinc oxide nanoparticles and studies of their catalytic activity towards ultrasound-assisted degradation of metronidazole", *Materials Letters 168*, 13 January 2016, pp 158-162.

[26] Gandhi V., Ganesan R., Syed Ahamed H. H. A., Thaiyan M., Effect of cobalt doping on structural, optical, and magnetic properties of ZnO nanoparticles synthesized by Co precipitation method, *Journal of Physical Chemistry C 118*, April 7, 2014 pp 9715-9725.

[27] Zak A. K., Majid W.H. Abd., Darroudi M., Yousefi R., "Synthesis and characterization of ZnO nanoparticles prepared in gelatin media", *Materials Letters 65*, 24 November 2010 pp70-73.

[28] Alias S.S., Ismail A.B., Mohamad A.A., "Effect of pH on ZnO nanoparticle properties synthesized by sol-gel centrifugation", *Journal of Alloys and Compounds 499*, 25 March 2010, pp 231-237.

[29] Thapa D., Huso J., Morrison J. L., Corolewski C. D., Mc Cluskey M. D., Bergman L., "Achieving highly-enhanced UV photoluminescence and its origin in ZnO nanocrystalline films", *Optical Materials 58*, 14 June 2016, pp 382-389.

[30] Ahn H.C., Kim Y.Y., Kim D.C., Mohanta S.K., Cho H.K., "A comparative analysis of deeplevel emission in ZnO layers deposited by various methods", *Journal of Applied Physics 105*, 05 January 2009, 01.